Tu-AM-I7

IMMUNOLOCALIZATION OF THE mNa$_v$2.3 Na^+ CHANNEL IN HEART AND UTERUS. ((T.J. Knittle, K.L. Doyle, and M.M. Tamkun)) Dept. of Molecular Physiology and Biophysics, Vanderbilt Medical School, Nashville, TN 37232.

mNav2.3 is a putative voltage-gated Na^+ channel (NaCh) expressed in heart and uterus that shares only 45% amino acid sequence identity with NaChs from gene subfamily 1. Northern analysis revealed that mNav2.3 is the only cloned NaCh expressed in mouse uterus and the levels of mRNA significantly increased during the latter stage of gestation. To examine the cell-specific expression of mNav2.3 protein in mouse heart and uterus during gestation, rabbit polyclonal antibodies were raised against bacterially produced fusion proteins containing unique mNav2.3 sequence from the carboxyl terminus and the cytoplasmic linker connecting domains 2 and 3. Immunohistochemical (IHC) studies revealed that mNav2.3 expression in heart and quiescent uterus colocalized with only glial and nerve-specific antibodies. During late pregnancy, mNav2.3 expression in nerve disappeared concomitant with increased expression in both longitudinal and circular smooth muscle. Expression in uterine myocytes reached a maximum at term and quickly declined after delivery. In all experiments, identical IHC patterns were observed with antisera raised against both epitopes. IHC results are supported by Western analysis in which the 217 kDa NaCh increased during late pregnancy. These data are consistent with reported increases in uterine myocyte NaCh density during pregnancy. It is likely that mNav2.3 is the uterine NaCh first reported by Sperelakis et al. The function of mNav2.3 expression in the uterus during gestation and delivery remains to be determined.

Tu-AM-I8

DIFFERENTIAL EFFECT OF HALOTHANE ON Na^+ AND Ca^{2+} CHANNELS EXPRESSED IN *XENOPUS* OOCYTES. ((A. M. Correa and N. Qin)) Dept. of Anesthesiology, UCLA, Los Angeles, CA, 90024.

General anesthetics (GA) modify cell excitability in nerves and muscles by differential effects on ligand-gated and/or voltage-gated ion channels. The basic mechanisms involved are still unclear. The purpose of this work was to examine in detail the properties of V-dependent ion channels exposed to volatile anesthetics. The cut open oocyte technique was used to look at the effects of Halothane (**Hal**) on the kinetics and conductance properties of Na^+ and Ca^{2+} channels. *Xenopus* oocytes were injected with cRNA's encoding for the alpha (α) subunits of the skeletal muscle Na^+ channel (μI) and of the cardiac (α1C, N60 an N-terminal truncation) Ca^{2+} channels. Currents were recorded from oocytes expressing α subunits alone and α plus beta (β) subunits (β_1 for μI Na^+ and β_{1b} or β_{2a} for Ca^{2+} channels). Perfusates were pre-equilibrated (15-20 min) with **Hal** vaporized at 3% in O_2. I_{Na} currents were recorded in external 120 NaMES and internal 90 Cs_2SO_4. I_{Ca} currents were recorded in external 10 BaMES, 96 NaMES and internal 120 KMES. **Hal** did not affect the magnitude of Na^+ currents. There was no change in the slope conductance (G = 20 mS for α and 78 mS for $\alpha+\beta$) nor in the V-dependence of the peak I or of the fractional conductance. Only minor changes in kinetics were observed: activation and inactivation were faster than control. Conversely, Ca^{2+} currents were blocked $\simeq$50% with no apparent shift in the V-dependence of the current or of the fractional conductance. Results are consistent with L-type Ca^{2+} channel block by **Hal**. **Hal** also shifted the relative contribution of fast and slow components of α1C currents. The effects on I_{Na} and I_{Ca} currents did not depend on β subunits coexpression. These results support specific interactions of channel proteins with GA. NQ supported by NIH AR43411.

Tu-AM-I9

BIOFERROELECTRICITY IN THE SODIUM CHANNEL: CONFORMATIONAL CHANGE IN THE PROBABLE ACTIVE SITE. ((Vladimir S. Bystrov and H. Richard Leuchtag)) Institute of Mathematical Problems of Biology, Russian Academy of Sciences, Pushchino, 142292, Russia, and Department of Biology, Texas Southern University, Houston, TX 77004. (Spon. by M. Hillar)

The closed Na channel is in a nonequilibrium state due to the strong field of the resting potential. Depolarization leads to a transition to an ion-conducting open state. Interpretation of the transition as ferroelectric-paraelectric explains a number of electrical and thermal phenomena. The hypothesis is completed by the assumption that the open channel is a superionic conductor. The inward movement of this phase transition has been studied by a thermodynamic ferroactive model. The equation of motion yields a kink solution for the transition front. The primary structure of the Na channel suggests that the four S4 segments of the channel, acting as a unit, form the active site involved in voltage sensing and ion conduction. Electrostatic analysis shows that an S4 segment is unstable as an α helix without external forces, suggesting that the resting potential induces these forces. On depolarization the S4s are postulated to extend and become coordinated by mobile ions traversing them.

Tu-AM-I10

BIOFERROELECTRICITY IN THE SODIUM CHANNEL: MOLECULAR TILT AND CHIRALITY. ((H. Richard Leuchtag)) Department of Biology, Texas Southern University, Houston, TX 77004.

Ion channels are molecular components of membranes, which have the two-dimensional order of lyotropic smectic liquid crystals. The hypothesis of a ferroelectric unit in a sodium channel, which provides physical explanations for the open-closed transitions, gating currents and thermal phenomena, thus suggests a comparison with ferroelectric liquid crystals. These are known to be of the smectic C* type: elongated chiral molecules that are tilted at an angle to the layer normal. Since the probable active site and ferroelectric unit is the four-S4 bundle, the question becomes whether the S4s are tilted and the bundle chiral. Potassium-channel and other studies suggest a tilt of the S4 segments, and the conserved proline residues present in three of the Na-channel S4s bend the α helices, providing the necessary chirality. Thus the closed channel appears to satisfy the necessary conditions to be a component of a smectic C* ferroelectric liquid crystal. An electric-field-induced transition may then unwind the α helices, breaking their H bonds, to establish a new paraelectric structure coordinated by the permeant ions, the open channel.

EMULATION AND SIMULATION OF NEURONAL FUNCTION

Tu-PM-Sym-1

MODELLING AND MEASURING CA^{2+} DYNAMICS IN NEURONAL SIGNALLING. ((D.W. Tank)) AT&T Bell Labs., Murray Hill, NJ

Tu-PM-Sym-2

USE OF THE DYNAMIC CLAMP TO MODULATE NEURONS AND NETWORKS. ((E. Marder)) Brandeis Univ.

Tu-PM-Sym-3

EMULATING NEURAL DECODERS: LEARNING TO READ NEURONAL SPIKE TRAINS. ((J.P. Miller)) Univ. of California, Berkeley.

Tu-PM-Sym-4

VSLI AND THE SILICON NEURON. (C. Mead)) California Inst. of Technol.

Na/Ca EXCHANGE AND E-C COUPLING

Tu-PM-A1

NA-CA EXCHANGE TRIGGERS CONTRACTION IN RAT VENTRICULAR MYOCYTES. ((J. Andrew Wasserstrom and AnaMaría Vites)) Department of Medicine, Northwestern University Medical School, Chicago, IL, 60611.

It has recently been reported that Na-Ca exchange triggers Ca^{2+}-induced Ca^{2+} release (CICR) and contraction in cat and guinea pig but not in rat ventricular myocytes. We used the whole cell voltage clamp technique at 34°C to study the role of Na-Ca exchange in triggering contraction in isolated rat ventricular myocytes. Pipette solution contained 6mM Na^+, 50μM EGTA, 4mM ATP and 153mM K^+. Rat myocytes demonstrated phasic cell shortening in response to voltage steps from -70 to -40mV. Cell shortening was decreased only slightly by addition of nifedipine (2-5μM) to the external solution. Contraction amplitude increased in response to test voltage steps between -30 and +10mV but then declined only slightly at test voltages up to +100mV; these contractions were decreased but not abolished by exposure to nifedipine. Addition of saxitoxin (STX, 2-3μM) usually, but not always, blocked cell shortening in response to these voltage steps. When contraction was activated by a voltage step mimicking the rat ventricular action potential, nifedipine again had only a slight negative inotropic effect. Our results demonstrate that 1) Na^+ influx via fast Na^+ current activates reverse mode Na-Ca exchange that provides sufficient Ca^{2+} influx to trigger CICR and phasic contraction in rat ventricular myocytes; 2) voltage-dependent Na-Ca exchange transports sufficient Ca^{2+} into rat myocytes to activate CICR and contraction even at potentials too positive for passive Na^+ and Ca^{2+} influx via their respective ion channels; and 3) activation of contraction at near-physiological conditions (34°C, no Na^+_i overload, action potential stimulus) relies at least in part on Ca^{2+} influx via Na-Ca exchange in rat ventricular myocytes.
Supported by grants from the NIH and the Chicago Affiliate of the AHA.

Tu-PM-A2

CALCIUM INFLUX VIA Na/Ca EXCHANGE AND CALCIUM CURRENT CAN BOTH TRIGGER TRANSIENT CONTRACTIONS IN CAT VENTRICULAR MYOCYTES ((Ana-María Vites and J. Andrew Wasserstrom)) Dept. of Medicine, Northwestern University Medical School, Chicago, IL 60611

We investigated the possibility that Ca^{2+} entry via the reverse mode of the Na/Ca exchanger can trigger transient contractions mediated via Ca^{2+}-induced Ca^{2+} release (CICR) from the sarcoplasmic reticulum in isolated cat ventricular myocytes (T=34°C). Membrane current, voltage, myocyte shortening (ΔL) and rate of shortening (dL/dt) were measured under voltage clamp conditions. Test voltage steps (V_t) from a holding potential of -40mV to a voltage range of -20mV to +120mV were used to produce ΔL activated by either I_{Ca} or reverse Na/Ca exchange. The voltage dependence of ΔL and dL/dt peaked at approx. +10mV and decreased at higher voltages, reaching a minimum at approx. -50mV. This was followed by a second phase of increased ΔL and dL/dt at V_t positive to +70mV. We observed no difference between I_{Ca}- and Na/Ca exchange-mediated cell shortening. However, we did observe a slower rate of relaxation of exchange-mediated ΔL when the duration of V_t was greater than 170msec. Nifedipine (3-10μM) and Ni^{2+} (1-2mM) blocked I_{Ca}- and exchange-mediated cell shortening, respectively. Ryanodine prevented all transient contractions, confirming that they result from CICR and not from direct activation of the myofilaments by Ca^{2+} originating from transmembrane Ca^{2+} influx. We conclude that Ca^{2+} entry via Na/Ca exchange is an effective mechanism to trigger fast CICR in heart. Therefore, reverse Na/Ca exchange should also be considered to be a mechanism that participates in cardiac E-C coupling.
(Supported by the NIH and the Chicago Affiliate of the AHA.)

Tu-PM-A3

FURTHER EVIDENCE THAT REVERSE NA-CA EXCHANGE CAN TRIGGER SR CALCIUM RELEASE. ((S.E. Litwin, G. S. Webster, J.H.B. Bridge.)) University of Utah, Salt Lake City, UT.

We measured I_{Ca} and the rate of phasic cell shortening triggered by sarcoplasmic reticulum (SR) Ca^{2+} release in isolated rabbit ventricular myocytes (n= 45) under voltage clamp conditions (V_{hold}=- 40 mV, 2.7 mM Ca^{2+} in bath at 30° C). Suction pipettes (1-2 MΩ) contained 0, 10, or 15 mM Na. I_{Ca} and peak shortening rates were normalized to their values at +10 mV. At each pipette [Na], I_{Ca} declined at membrane potentials greater than +10 mV to a greater extent than did shortening rate. Shortening rate at potentials > 10 mV was strongly affected by pipette [Na] (Fig A). We blocked I_{Ca} by rapid application of nifedipine (20 µM) 6 sec before test pulses (pip Na = 10 mM) (Fig B). The nifedipine-sensitive shortening rate declined at potentials > +10 mV; whereas, the nifedipine-insensitive shortening rate increased at these potentials.

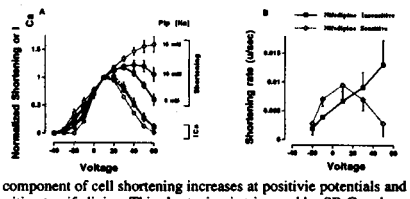

In summary, a component of cell shortening increases at positivie potentials and is sensitive to $[Na]_i$, but insensitive to nifedipine. This shortening is triggered by SR Ca release because it is abolished by ryanodine and thapsigargin in the presence of nifedipine. We conclude that Na_i-dependent cell shortening is produced by SR Ca release triggered by reverse Na-Ca exchange.

Tu-PM-A4

TEMPERATURE ALTERS Ca TRANSPORT RATE DURING RELAXATION IN CARDIAC MYOCYTES, BUT NOT THE RELATIVE ROLES OF THE SR Ca-PUMP AND Na/Ca EXCHANGE. ((J.L. Puglisi, R.A. Bassani, J.W.M. Bassani, J.N. Amin and D.M. Bers)) Loyola University Chicago, Maywood, IL 60153.

We have previously analyzed the quantitative contributions of four Ca transport systems to the removal of Ca from the cytoplasm during relaxation of cardiac myocytes at room temperature (SR Ca-pump, Na/Ca exchange, sarcolemmal Ca-pump and mitochondria, with the latter two lumped as "slow" systems: *J. Physiol.* 453:591, 1992; 476:279-293, 1994). Here we assess the influence of temperature on this competition in different species. We define the ratio of t½ for relaxation at 25°C to 35°C as the "T_{10}". For rabbit, cat and ferret respectively T_{10} for twitches was 2.6, 2.6 & 2.4. Similarly, the T_{10} for caffeine-induced contractures (CafC), where relaxation is primarily due to Na/Ca exchange was 1.9, 1.8 & 2.5. For relaxation due to the slow systems (CafC in 0Na, 0Ca) the T_{10} was 3.4, 2.3 & 1.8. Thus, all the systems are faster at 35°C than 25°C. The relative effect was studied in more quantitative detail in rabbit myocytes with $[Ca]_i$ measurements during twitches and CafC in control or 0Na, 0Ca solution. The figure shows the analysis of the relative contributions of the systems as a running integral of Ca transport during relaxation. While each system becomes faster, the relative contribution to relaxation is not much altered.

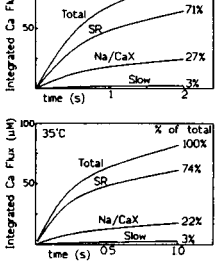

Tu-PM-A5

RELAXATION IN FERRET VENTRICULAR MYOCYTES: ROLE OF THE SARCOLEMMAL (SL) Ca-ATPase ((R.A. Bassani, J.W.M. Bassani and D.M. Bers)) Loyola Univ Chicago, Maywood, IL 60153. Spon. by T. Shannon.

In ferret ventricular myocytes relaxation and the rate of $[Ca]_i$ decline when SR Ca accumulation and Na/Ca exchange are inhibited (10 mM caffeine in 0Na,0Ca solution) is 3-4 times faster than in rabbit and rat myocytes. In this study, we investigated the role of the SL Ca-ATPase in this process, using a novel approach to inhibit this pump in intact myocytes, namely intracellular loading with an esterified form of carboxyeosin (C-Eosin, Gatto & Milanick, *Am J Physiol* 264:C1577, 1993). The ability of C-Eosin to change the time-course of $[Ca]_i$ decline was compared to that of increased $[Ca]_o$ (10 mM) in rabbit and ferret myocytes. In rabbit cells, both procedures produced similar effects, and additional inhibition of mitochondrial Ca uptake virtually abolished $[Ca]_i$ decline. In ferret cells, C-Eosin treatment, produced these same effects on $[Ca]_i$ decline, but high $[Ca]_o$ did not mimic them. Moreover, only in C-Eosin-treated ferret cells did additional inhibition of mitochondrial Ca uptake nearly abolish $[Ca]_i$ decline. We concluded that: a) C-Eosin loading is a useful procedure to inhibit the SL Ca-ATPase in intact myocytes; b) this pump seems likely to be responsible for the much faster relaxation observed in ferret cells after block of SR Ca accumulation and Na/Ca exchange transport; c) the SL Ca-pump apparently has different kinetic characteristics in rabbit and ferret ventricular myocytes.

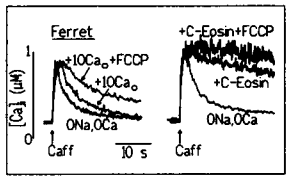

Tu-PM-A6

CLONING OF THE cDNA OF THE FROG HEART SARCOLEMMAL Na^+-Ca^{2+} EXCHANGER. ((T. Iwata, A. Kraev, M. Morad and E. Carafoli)) Institute of Biochemistry, Swiss Federal Institute of Technology (ETH), 8092 Zurich, Switzerland; and Department of Pharmacology, Georgetown University, Washington, DC 20007. (Spon. by G. Langer)

The cardiac sarcolemmal Na^+-Ca^{2+} exchanger is essential for the regulation of the heart contraction/relaxation cycle. The Na^+-Ca^{2+} exchanger cDNA clones have been isolated from various tissues and species. A second exchanger gene has been recently identified in rat. All isoforms coded for the NCX1 genes are conserved well across species and tissues, except for variations caused by alternative splicing of the primary transcript at a site in the main intracellular loop. Numerous isoforms, differing in a small portion of the large intracellular loop of NCX1 gene are produced by different splicing of several small exons. Mammalian heart is known to express predominantly one isoform, utilizing certain exons, not found in other tissue-specific isoforms. Here we report the cloning of the Na^+-Ca^{2+} exchanger cDNA in the frog heart. The clone was found to be the product of the NCX1 gene and its sequence was well conserved with respect to other species, especially in the transmembrane domains. But significant differences were found in the intracellular loop. In particular, an extra sequence of nine amino acids was found in a clone at the site where the alternative splicing occurs in the intracellular loop in other species. Since the insertion of this domain did not change the reading frame, it seems likely that this stretch should be coded by a novel exon, so far not found in the mammalian heart. Since this portion of the intracellular loop is thought to serve as a regulatory site of the protein, it may provide the molecular site for the regulatory action of β-adrenergic modulation of the Na^+-Ca^{2+} exchanger current via PKA phosphorylation, recently found in the frog heart.

Tu-PM-A7

MODULATION OF SODIUM-CALCIUM EXCHANGER BY BETA-ADRENERGIC AGONISTS IN FROG VENTRICULAR MYOCYTES. ((J. Fan, Y. Shuba, and M. Morad)) Department of Pharmacology, Georgetown University, Washington, DC 20007.

β-agonists enhance myocardial twitch but suppress KCl or voltage-clamp induced contracture tensions in mammalian and frog heart. Phosphorylation of phospholamban and stimulation of SR Ca-ATPase in mammalian heart mediate the relaxant effects of β-agonists. The absence of SR Ca-ATPase and its mRNA in frog heart (Kurebayashi et al JMCC, 1994; Vilsen et al FEBS letters 306, 1992) makes it unlikely that the β-agonist contracture-suppressant effect is caused by phosphorylation of phospholamban. We examined the possible role of Na^+-Ca^{2+} exchanger in mediating the contracture relaxant property of isoproterenol (ISO). Isolated, whole cell clamped, frog myocytes were dialyzed with high CsCl or KCl, 10-20mM Na^+, 0.1mM BAPTA, and 0.2mM EGTA. Nifedipine, Ba^{2+}, and TEA were used to block the I_{Ca}, I_{K1} and I_K respectively. The slowly decaying outward current at +20 to +80mV and the tail currents upon repolarization at -80mV was identified as $I_{Na\text{-}Ca}$. 3mM Ni^{2+} rapidly and reversibly blocked these currents and suppressed the contraction. Repolarizing ramp clamps from +80mV to -120mV were used to measure voltage-dependence of $I_{Na\text{-}Ca}$. 5μM ISO within 60s suppressed cell shortening and $I_{Na\text{-}Ca}$ by 50-80% and shifted the $I_{Na\text{-}Ca}$ reversal potential by -20mV, suggesting significant reduction of $[Ca^{2+}]_i$. Propranolol blocked and 100μM 8-Br-cAMP, 10μM forskolin, and 2mM theophylline mimicked the ISO effects on $I_{Na\text{-}Ca}$ and contraction. The data suggest that ISO regulates Na^+-Ca^{2+} exchanger protein via the β-receptor adenylate cyclase pathway providing a novel molecular mechanism for the contracture-suppressant (relaxant) property of β-agonists in frog heart. Supported by NIH HL16152.

Tu-PM-A8

Abstract Withdrawn.

Tu-PM-A9 *(See Tu-Pos220)*

K^+ CHANNEL GATING

Tu-PM-B1

DISCRIMINATION BETWEEN ACTIVATION MODELS FOR *SHAKER* POTASSIUM CHANNELS ((N. E. Schoppa and F. J. Sigworth)) Department of Cellular and Molecular Physiology, Yale Univ., New Haven, CT 06510. (Spon. by D.-S. Jong)

Several activation models for *Shaker* have been proposed (e.g., Zagotta et al., *J Gen. Phys.* 103, 321 (1994) and Bezanilla et al., *Biophys. J.* 66, 1011(1994)). To address issues raised by these efforts, we report our own experiments with the normally activating *Sh* 29-4 channel (WT) and a channel (V2) with the mutation L382V in the *Sh* B sequence, which alters channel opening but has little effect on the channel's charge movement (Schoppa, McCormack, et. al., *Science* 255, 1712 (1992)):

(1) What accounts for *Sh*'s slow deactivation? Analysis of transitions near the open state show that the closing WT reopens frequently (~7 times at -50 mV where τ_{tail}~20 ms) before closing to earlier states. This behavior appears to be mediated by two unique final transitions: from analysis of WT's "off" gating currents, the deactivation kinetics associated with the final two transitions are much slower than that associated with all earlier transitions; also, V2 alters and only alters the final two transitions.

(2) What accounts for *Sh*'s slow activation and the observed associated slow charge movement (Q_{open}) present at its activation voltages (near -30 mV)? Two explanations are a slow, large-valence channel opening step or, alternatively, early unfavorable transitions combined with a favorable final step which pulls channels via mass action into the open state. Evidence for the latter is that V2, which does not open, and lacks WT's Q_{open} at -30 mV, lacks a large Q_{open} at its own activation voltages.

(3) Is there cooperativity between subunits? Maybe not, insofar as many of the transition forward and backward rates appear to be similar.

Finally, we propose a model : $(S_0 \leftrightarrow S_1 \leftrightarrow S_2)_4 \leftrightarrow C \leftrightarrow O \leftrightarrow C$.

The channel opens after each of four subunits undergoes two transitions in sequence, and following two more concerted conformational changes.

Tu-PM-B2

ROLE OF THE S5 REGION OF SHAKER K^+ CHANNEL IN THE MOVEMENT OF THE VOLTAGE GATE AND ITS INTERACTION WITH THE OPEN PORE ((Max Kanevsky and Richard W. Aldrich)) Dept. of Molecular and Cellular Physiology and Howard Hughes Medical Institute, Stanford University School of Medicine, Stanford, CA 94305.

The best-known *Shaker* allele with a novel gating phenotype, Sh^5, differs from wild type by a subtle point change (F401I) in the putative S5 transmembrane segment (Gautam & Tanouye, 1990; Lichtinghagen *et al.*, 1990). Kinetic analysis of this mutant revealed that changes in the deactivation rate could account for the altered gating behavior (Zagotta & Aldrich, 1990), although closing kinetics and steady-state activation could not be directly assessed in the presence of intact fast inactivation. The Sh^5 results led us to ask whether systematic changes to the gating mechanism could be obtained by making conservative substitutions at position 401 and at other aromatic amino acids in S5. Mutations of F401 to I, V and A, when expressed in the ShB background with disrupted N-type inactivation, produced currents that were characterized by decreased apparent voltage dependence and accelerated activation and deactivation kinetics. These changes correlated with decreasing bulk of the side chain. Substitution F401A gave rise to channels with extremely shallow voltage dependence: whereas activation began in the wild type range (ca. -40 mV), the conductance-voltage curve did not saturate at voltage up to 200 mV. In F401A, gating currents show that the rise in the open probability with voltage lags far behind charge movement. In wild type channels, the subunits' active conformation displays cooperative stabilization which may come from interaction with the open pore (Zagotta *et al.*, 1994). Measurements of macroscopic deactivation, single-channel open times, current sigmoidicity as well as data from Cole-Moore experiments indicate that F401 mutants lose this form of cooperativity. At other sites in S5, phenylalanines do not play equivalent roles in voltage-dependent gating, consistent with the model that some (F401) may stabilize a voltage-sensing positive residue in the active conformation whereas others (F416) may have similar interaction with a residue outside of the electric field.

Tu-PM-B3

EXPLORING THE ROLE OF THE S4-S5 LINKER REGION IN THE ACTIVATION MECHANISM OF *SHAKER* POTASSIUM CHANNELS. ((Z.-J. Xu and R. W. Aldrich)) Howard Hughes Medical Institute and Department of Molecular and Cellular Physiology, Stanford University School of Medicine, Stanford, CA 94305.

Activation properties were studied in chimeric channels constructed using the non-inactivating *ShakerB* channel mutant (*ShB*Δ6-46) as the background and substituting the S4-S5 linker region from several divergent potassium channels including *fShab, DRK1, fShal, fShaw* or *RKShIIIA*. The channels were expressed in *Xenopus* oocytes and recorded with the patch-clamp and the cut-open oocyte voltage clamp techniques. The macroscopic currents of all the chimeras have a similar time course of activation as the *ShB*Δ6-46 channels. Chimeras with the *Shab* or *DRK1* linker insert have steeper and negatively shifted conductance-voltage (GV) curves accompanied by slower tail current kinetics compared to that of *ShB*Δ6-46. In contrast, the chimera with *Shaw* linker insert has a much shallower and positively shifted GV curve, and the tail currents are much faster. The gating currents of *ShB*Δ6-46, *Shab* linker and *Shaw* linker chimeras were studied either by blocking the ionic currents with Agitoxin or in the non-conducting mutants of these channels resulting from a tryptophan to phenylalanine substitution at amino acid 434 (Perozo et al, Neuron, 11 : 353-358). The *Shab* linker chimera has a similar QV curve as *ShB*Δ6-46, but the QV curve for *Shaw* linker chimera is shallower. The distance along the voltage axis between QV and GV curves is widened for *Shaw* linker chimera compared to that for *ShB*Δ6-46. The QV and GV curves for *Shaw* linker chimera, however, reside very closely to each other. The speed of decay of the off gating current is increased in *Shaw* but decreased in *Shab* linker chimera. These results are consistent with a view that the S4-S5 linker region is closely associated with the charge movement. In addition, this region may play a role in stabilizing the channel in the open state.

Tu-PM-B4

GATING CURRENTS OF ACIDIC RESIDUES MUTANTS IN *SHAKER* K+ CHANNEL. ((F. Bezanilla, Sang Ah Seoh and D. M. Papazian)). Dept. of Physiology, UCLA, Los Angeles, CA 90024.

Much attention has been paid to the S4 segment as a possible site for the voltage sensor in Na, K and Ca channels because it contains a series of positively charged amino acids. However, the role of negative charges has not been investigated in any detail, although it has been generally thought that they could act as counter charges for the residues in the S4 or even be part of the voltage sensor. Using the cut-open oocyte technique we have studied the effects of neutralizations of positions E283, E293 and D316 on the gating currents of *Shaker* B in constructs with fast inactivation removed (IR) and with the pore mutation W434F that renders them non-conductive. All three mutations show drastic changes in kinetics and steady-state properties. E283Q exhibits a shift of the Q-V to the right but maintains the valence and proportions of the two gating components. The Q-V of E293Q saturates near 0 mV and the currents shows slow ON kinetics and extremely slow OFF kinetics. The Q-V curve of D316N exhibits a shift to the right for both gating components. The second component of D316N is shifted by about 50 mV and the apparent valence decreased to about 2. D316N resembles the S4 mutant R368Q but the separation of the charges is not as large and it seems to saturate near +60 mV. These results indicate that acidic residues E283, E293 and D316 participate in the charge rearrangements leading to channel activation. Of particular interest is position D316 which upon neutralization makes the second component of charge shallower and decreases the proportion of the second to the first component, indicating that this residue might be part of the voltage sensor. E283 and E293 are in segment S2 while D316 lies in segment S3. If segments S3 and S4 are alpha helices, their dipole moments would be anti-parallel and it is conceivable that they would form a basic sensing dipole. Supported by UPHS grants GM43459 and GM30376.

Tu-PM-B5

TEMPERATURE DEPENDENCE OF GATING CURRENT (Ig) IN SHAKER B K+-CHANNEL. ((B.M. Rodriguez, Sigg, D. and F. Bezanilla)). UCLA. Dept. of Physiol. Los Angeles, Ca 90024. USA. (Sponsored by E. Perozo).

Ig from noninactivating and nonconducting Shaker K^+-channels were expressed in *Xenopus* oocytes and recorded with the Cut-Open Oocyte Voltage Clamp. Steady-state and kinetic properties were studied between 3 and 22 °C. The On and Off responses were described by a rising phase followed by fast and slow decaying components. A linear Arrhenius plot can describe the temperature dependence of the fast component in the On and Off responses (Q_{10}> 2.6, at -10 mV and -60 mV). In general, at both potentials, for the rising phase and the slow decaying component, two lines were required to fit the Arrhenius plot (between 22- 8 °C, Q_{10} > 2.3 and between 8- 3 °C, Q_{10} > 6.1). The slow component for the On is the most temperature-dependent, with a large entropic change during the process. In a two-pulse experiment the rate of recovery at -90 mV from a pre-pulse at -50 mV has a Q_{10}= 1.3 ± 0.1 (n=2), but when recovering from 0 mV the Q_{10} is 4.0 ± 0.34 (n=2). These results agree with the idea that initial transitions involve multiple steps with low energy barriers, whereas later transitions involve few steps with high energy barriers. The charge (Q) versus potential (V) curve reveals a reversible decrease in charge movement at low temperature (20 % at 3 °C). The Q-V curve shows two components of charge. The first ($V_{1/2}$= -61.6 ± 2.4 mV, n= 4, 20-22 °C) is shifted approx. -7 mV at 6 °C and -14 mV at 3 °C and the second ($V_{1/2}$= -40.3 ± 2.8 mV, n=4, 20-22 °C) does not show any shift. Noise analysis studies with the macropatch technique suggest neither the number of channels nor the unitary gating charge movement changes at low temperatures. However, the Open probability decreases by 14 % while the unitary conductance decreases by 33 % at temperature below 8 °C. This work was supported by USPHS grant GM30376 and BID-CONICIT and IVIC fellowships (from Venezuela).

Tu-PM-B6

FAST INACTIVATION OF IONIC CURRENTS AND "CHARGE IMMOBILIZATION" OF *SHAKER* H4 AND *Sh*H4 W434F K+ CHANNELS. ((M.J. Roux, L. Toro, E. Stefani)) Department of Anesthesiology, UCLA School of Medicine, Los Angeles, CA 90024.

We introduced the pore mutation W434F in *Shaker* H4 K^+ channel, which in H4IR clone prevents ionic conduction without affecting the gating currents (I_g). The *Sh*H4 and *Sh*H4 W434F clones were expressed in *Xenopus* oocytes. I_g (*Sh*H4 W434F) and ionic currents (I_i) (*Sh*H4) were recorded with the COVG technique. The *Sh*H4 W434F channel displays ON gating currents similar to *Sh*H4IR W434F. The OFF gating currents, on the other hand, were dramatically slowed down for depolarizing pulses that open the channel. This indicates that the inactivation "ball" is still able to bind to its site in the *Sh*H4 W434F mutant and slows down the charge return. The time course of recovery from fast inactivation was monitored at different post-pulse potentials (-120, -90, -70 and -50 mV) after a 50 ms test pulse to 20 mV, in the *Sh*H4 W434F clone for I_g and in the *Sh*H4 clone for I_i. Both I_g and I_i have at least two components in the recovery process. At -120 mV both I_g and I_i followed a similar time course. On the other hand, for the other more positive potentials, the full recovery is reached faster for I_i than for I_g. This can be tentatively explained if K^+ ions in the conducting pathway of the *Sh*H4 destabilize the "ball" docking to the channel. In the *Sh*H4 W434F mutant, this effect would not be present due to the lack of K^+ in the pore or due to slight changes in the docking site.
Supported by NIH grants, GM50550 to ES and LT.

Tu-PM-B7

ELECTROSTATIC INTERACTIONS OF S4 VOLTAGE SENSOR IN SHAKER K+ CHANNEL. ((D.M. Papazian, X.M. Shao, S.-A. Seoh, A.F. Mock, Y. Huang, and D. Wainstock)), Department of Physiology, UCLA School of Medicine, Los Angeles, CA, 90024.

The S4 segment comprises part of the voltage sensor in Shaker K^+ channels. Two S4 neutralizations, K374Q and R377Q, block maturation of the Shaker protein. This suggests that they disrupt electrostatic interactions with transmembrane acidic residues that are important for the channel's tertiary structure. To test this hypothesis, the S4 mutations were individually paired with neutralization mutations in the following conserved residues: E283 and E293 in S2, D316 in S3, and D447 in the P region. Pairing K374Q with E293Q or D316N restored efficient maturation and generated high levels of functional activity. Pairing K374Q with E283Q or R377Q with E283Q, E293Q, or D316N rescued poorly, leading to inefficient maturation and low levels of functional activity. In contrast, D447N did not rescue the defects in K374Q or R377Q. These results suggest that K374 and R377 in the S4 segment interact electrostatically with acidic residues in S2 and S3. Neutralizing an S4 residue makes it infeasible to fold the acidic residues into their normal positions in the structure. Adding a second neutralization in one of the acidic residues removes this barrier; other structural interactions are apparently then strong enough to generate the active structure. We interpret efficient rescue to indicate strong, short range electrostatic interactions, whereas poor rescue indicates longer range, weak electrostatic interactions. Because both E293Q and D316N rescue K374Q efficiently, K374, E293, and D316 may be part of a charge network. We can account for the effects of the double mutant combinations on the voltage dependence of activation with a simple structural model.

Tu-PM-B8

SUBCONDUCTANCE BEHAVIOR SUPPORTS A NEW MODEL FOR GATING AND PERMEATION OF K CHANNELS BASED ON SUBUNIT CONFORMATIONS. ((AMJ VanDongen and ML Chapman)) Dept of Pharmacol, Duke Univ Med Cntr, Durham NC 27710. (Spon. by N. Malouf)

Voltage dependent ion channels consist of subunits or domains surrounding a central ion conducting pore. In K channels the subunits are identical, therefore each subunit makes an identical contribution to the pore lining to define ion selectivity and permeation rate. Following activation of the channel, ion channels switch stochastically between an open and a closed state. During the transition between these two channel states, each subunits must move between a conformation that supports ion permeation and one that does not. If the subunits do not move in perfect synchrony, than the channel would be transiently in a heteromeric conformation, in which some subunits are "open" and others are "closed". Here we present evidence that some of these heteromeric channel conformations produce short-lived subconductance levels. A subunit-subconductance model is proposed, in which a subunit has 3 conformations: resting (R), active (A), or open (O). R and A describe the state of the voltage sensor (S4), and do not support permeation. The O state has a different pore conformation that supports permeation and can only be reached from the R state. A channel with four of these subunits has 15 different states, 9 of which have heteromeric pores. These heteromeric channel conformations are assumed to be short-lived, and some of them permeate ions, although at a rate less then the homomeric open channel. The model predicts that subconductance behavior should be abundant when channels are incompletely activated (i.e. a mixture of R and A). Experimental evidence from native and mutant K channels supports this idea. In the new model "gating" (open-close behavior) and permeation are tightly coupled.

Tu-PM-B9

THE CHARGE CONTENT OF THE S4 REGION IN EAG K^+ CHANNEL IS NOT SUFFICIENT TO DETERMINE ITS VOLTAGE-DEPENDENCE.
((Chih-Yung Tang and Diane M. Papazian)) Department of Physiology, UCLA School of Medicine, Los Angeles, CA 90024. (Spon. by Naomi Nagaya)

Drosophila eag K^+ channels (*eag*) and rat olfactory channels (Rolf) belong to the superfamily of voltage-gated channels. Because both contain a putative cyclic nucleotide-binding domain, they are more closely related to each other than they are to the 4 subfamilies of voltage-gated K^+ channels. The *eag* K^+ channel is voltage-dependent whereas Rolf is not, and yet both have an S4 segment, which comprises part of the voltage sensor in other voltage-gated channels. The *eag* S4 contains 7 positive charges and 2 negative charges (net charge +5), whereas the Rolf S4 contains 4 positive charges and 3 negative charges (net charge +1), leading to the hypothesis that this difference in S4 charge is responsible for the two channels having different voltage-sensitivities. To test this hypothesis, we replaced the S4 region of *eag* with that of Rolf. In one chimera, only the 5 most divergent residues were swapped, reducing the net charge on S4 to +2. In another chimera, most of the S4 residues (14 amino acids) were exchanged, reducing the net charge on S4 to +1. After expression in *Xenopus* oocytes, the voltage-dependence of the chimeric channels was determined by fitting the steady-state g-V curve with a simple Boltzmann distribution. Both chimeras were voltage-dependent, exhibiting slope parameters similar to that of wild-type *eag*, and right-shifted midpoint potentials. These results indicate that, at least in *eag*, the charge content of the S4 region is not sufficient to determine the channel's voltage-dependence. This conclusion contrasts with that of a previous report (Logothetis et al., *Neuron* 10:1121, 1993), involving chimeras between two voltage-gated K^+ channels, RCK1 and Shab11. Additional chimeras will be used to identify regions of the protein outside the S4 segment that contribute to the voltage-dependent activation of *eag*.

Tu-PM-B10

A COMPARISON OF THE GATING CHARGE PER CHANNEL OF THE SHAKER AND DRK1 K^+ CHANNELS.
((Sanjay K. Aggarwal and Roderick MacKinnon)) Department of Neurobiology, Harvard Medical School, Boston, MA 02115.

The opening of the *Shaker* K^+ channel is more steeply voltage dependent than *drk1*. We examined whether differences in the gating charge per channel between these two channels may underlie this difference in voltage dependence. We have previously determined the gating charge per channel of the *Shaker* K^+ channel by recording the nonlinear membrane capacitance due to expressed channels in single oocytes, and then using a radiolabelled toxin to count the number of channels in these same oocytes (Biophys J. 66:136a, 1994). In order to study *drk1*, we modified its P-region to render it sensitive to toxin. Preliminary measurements indicate that *drk1* has a much smaller gating charge per channel than the *Shaker* K^+ channel.

NEW MICROSCOPIES

Tu-PM-C1

TWO-PHOTON EXCITATION IN FAST CONFOCAL AND IN 4Pi AND THETA CONFIGURATIONS.
((Ernst H.K. Stelzer)) European Molecular Biology Laboratory, Postfach 10.2209, D-69012 Heidelberg, Germany.

The main advantage of two-photon over single photon excitation is the volume confinement in the illumination process. It is used in a fast (15 images/second) confocal fluorescence microscope to record sections through living specimens. Other advantages are the excitation of many dyes and the ratio of almost two of illumination and emission wavelengths. The latter property can be taken advantage of in coherent microscopies (e.g. in 4Pi (A)). It improves the axial resolution and helps forming phase controlling feed back loops. A two-photon 4Pi(A) confocal theta microscope has no significant axial side lobes and provides an excellent axial z-discrimination. This is an important step towards far-field microscopy that is not diffraction limited but wavelength limited. A lower limit on 3D resolution of a light microscope can be found.

Tu-PM-C2

3D LOCALISATION OF SINGLE NUCLEAR PORE COMPLEXES BY HIGH RESOLUTION CONFOCAL IMAGING.
((Ulrich Kubitscheck, Peter Wedekind, and Reiner Peters)) Institut für Medizinische Physik und Biophysik der Universität, 48149 Münster, Germany

The nuclear pore complex (NPC), mediating the selective transport of macromolecules between nucleus and cytoplasm, measures 125 nm in diameter and 70 nm in length. We used high resolution confocal laser scanning microscopy to localise single fluorescently labelled NPCs. The plasma membrane of 3T3 cells was permeabilized with digitonin, and the NPC fluorescently labelled using the monoclonal antibody mAb 414. Stacks of optical sections of individual nuclei were generated by confocal imaging at high resolution. Single NPCs could be detected as bright diffraction limited spots. Centers of these spots were determined by a fit to a 3D Gaussian, employing in case of overlapping intensity distributions up to six Gaussians simultaneously. This yielded an accuracy of ±1 pixel, i.e. ±40 nm in x- and y-, and ±200 nm in z-direction. From these data 3D maps were created revealing the distribution of NPCs on the nuclear surface. In addition, the pair correlation function was calculated to distinguish between random distributions, and attractive or repulsive interactions among NPCs.

Tu-PM-C3

DETECTION AND TRACING OF SINGLE FLUORESCENCE LABELED LIPIDS AND ANTIBODIES IN SUPPORTED LIPID BILAYERS
((Th. Schmidt, G.J. Schütz, W. Baumgartner, H.J. Gruber and H. Schindler)) Institute for Biophysics, University of Linz, Altenberger Str. 69, 4040 Linz, Austria.

Single lipid molecules and antibodies, mono-labeled with the fluorescent dye tetramethylrhodamine are observed in supported lipid bilayers using sensitive fluorescence microscopy. Single fluorescent molecules are identified as quantal intensities with a signal-to-noise ratio of 2 to 5 depending on the illumination intensity and illumination time. The positions of single dyes are traced in successive images with a time resolution of 10ms to an accuracy of ~50nm. The observed motion agrees with a 2-dimensional random walk and diffusion constants of $(2.5 \pm 0.2)\ 10^{-8}\ cm^{-2}/s$ for lipids, and of $(0.6 \pm 0.2)\ 10^{-8}\ cm^{-2}/s$ for antibodies are determined. The antibodies were conjugated to lipids via flexible spacers. Single dye detection was possible for molar ratios of dye to lipid between 10^{-9} and 10^{-6}. The application of this new, least invasive technique to antibody- or ligand binding to native membranes is discussed and first examples are shown.
(Supported by the Austrian Research Funds, project S66/07)

Tu-PM-C4

BIOLOGICAL APPLICATIONS OF NEAR-FIELD MICROSCOPY

((Robert C. Dunn, Errol V. Allen and X. Sunney Xie)) Pacific Northwest Laboratory[1], P. O. Box 999, MS K2-14, Richland WA. 99352.

Recent advances in near-field optical microscopy offer exciting possibilities for conducting molecular spectroscopy at the nanometer dimension. The technique involves scanning a spot of light, of dimension much smaller than the optical wavelength, in close proximity to the surface of a sample. For biological applications, fluorescence measurements with near-field optics is particularly informative, providing spectroscopic information not accessible with other scanning probe techniques such as SEM, STM and AFM.

A few groups, including ours, have recently demonstrated the sensitivity of the near-field technique by imaging the fluorescence of single dye molecules with sub diffraction resolution. Furthermore, we have completed a study on the fluorescence lifetimes of single dye molecules by incorporating a picosecond time-correlated single photon counting ability into our microscope. This study demonstrated the feasibility of lifetime imaging with single molecule sensitivity, nanometric resolution, and picosecond temporal resolution. In our efforts to study photosynthetic membranes, we have imaged intact photosynthetic membrane fragments from the *Chlamydomonas reinhardtii* PSI - PSII doubly deficient C2 strain. Membrane fragments from this strain contain only the LHCII. The emission images reveal a homogeneous distribution of LHCII throughout the membrane fragments, in agreement with recent SEM results. Lifetimes were also measured at various points within the membrane fragements. These studies are aimed at spectroscopically mapping the photosynthetic membrane and further progress along these directions will be presented.

[1]Pacific Northwest Laboratory is a multiprogram national laboratory operated by Battelle Memorial Institute for the U.S. Department of Energy under contract DE-AC06-76RLO 1830.

Tu-PM-C5

LUMINESCENT PROBES FOR SOFT X-RAY MICROSCOPY. ((M. M. Moronne,[1] C. Larabell,[1] P. R. Selvin,[1] W. Meyer-Ilse,[1] and A. Irtel von Brenndorff[2])) [1]Lawrence Berkeley Laboratory, University of California, Berkeley, CA 94720, USA. and [2]Forschungseinrichtung Röntgenphysik, University of Göttingen, Geiststr. 11, 37073 Göttingen, Germany.

The complimentary development of high resolution zone plate lenses and intense, tunable, monochromatic x-ray sources has made possible the construction of soft x-ray microscopes with high resolving power. X-ray scanning and imaging microscopes are now capable of better than 50 nm resolution, with improvements expected to reach 20 nm in the near future. To take advantage of the high resolution offered by x-ray microscopy, labels for specific subcellular targets must be developed. In this context, we report recent results demonstrating the use of lanthanide loaded polychelate conjugated secondary antibody and avidin luminescence probes. Using the scanning x-ray microscope (STXM) at the National Synchrotron Light Source equipped with a low noise, high efficiency photo-avalanche diode detector for visible light single photon counting,[2] we have demonstrated that labels based on terbium and europium polychelates continue to yield useful luminescence even after 10^{11} rads of 3.15 nm soft x-rays. Initial attempts to label actin filaments in 3T3 fibroblasts using a rabbit anti-actin primary followed by a terbium conjugated goat anti-rabbit secondary, revealed filamentous structures indicative of actin visualization. However, significant non-specific labeling is evident (e.g., in cell nucleoli) such that further chemical modifications to improve probe specificity is required. Assuming that such problems can be overcome, it will ultimately be possible to do multiple simultaneous labeling using terbium and europium that have unique visible emission spectra.

Tu-PM-C6

MEASURING THE ELASTIC PROPERTIES OF BIOLOGICAL MATERIALS WITH THE ATOMIC FORCE MICROSCOPE (Manfred Radmacher, Monika Fritz, Paul K. Hansma, Dept. of Physics, University of California, Santa Barbara, CA 93106)

We have used an Atomic Force Microcope (AFM) to determine the elastic properties of biological samples. In a force curve the AFM tip, which is mounted on a soft cantilever spring is brought in contact with the sample and retracted again. This loading and unloading curves can be analyzed in terms of topography, adhesive forces, elastic and other properties of the sample. Here we focus on the elastic properties We present data of thin films of gelatin, in different media (like propanol and water) and thin films of the protein lysozyme adsorbed on mica. The Young's modulus of gelatin was determined to be 1 MPa in a 1:1 mixture of propanol and water. It is about 0.1 GPa in 95% propanol and becomes larger than 1GPa in pure propanol. The elasticity of lysozyme in physiological buffer was determined to be 0.5 GPa.

Tu-PM-C7

OBSERVATION OF PROTEIN ACTIVITY DURING HYDROLYSIS BY ATOMIC FORCE MICROSCOPY

Monika Fritz, Manfred Radmacher, Helen G. Hansma, Paul K. Hansma. Department of Physics, University of California, Santa Barbara, CA 93106

The height fluctuations of individual molecules of the protein lysozyme were measured with a time resolution of approximately 1 msec and a height resolution of approximately 0.1 nm with an Atomic Force Microscope (AFM) operated in tapping mode in liquid. Height fluctuations of order 1 nm lasting for times of order 50 msec were observed over some lysozyme molecules when an oligoglycoside that is hydrolyzed by lysozyme was present in the liquid. These height fluctuations decreased to the level without the oligoglycoside if the lysozyme was inhibited with chitobiose. The most straightforward interpretation is that the height fluctuations correspond to the conformational changes of lysozyme during hydrolysis. It is also, however, possible that the height fluctuations are, at least in part, due to a different height or elasticity of the transient complex of lysozyme plus the substrate. In any case, the AFM could monitor the hydrolysis of a substrate by its enzyme by measuring the height fluctuations while sitting on top of the enzyme. This opens a new field of observing processes at a molecular level.

Tu-PM-C8

ATOMIC FORCE MICROSCOPY REVEALS TWO SIDES AND TWO CONFORMATIONS OF THE *E. COLI* OUTER MEMBRANE PORIN OMPF RECONSTITUTED IN THE LIPID BILAYER. ((F. A. Schabert, C. Henn and A. Engel)) Maurice E. Mueller-Institute, Biozentrum, Universität Basel, CH-4056 Basel, Switzerland. (Sponsored by M. Lösche)

Topographs of two-dimensional porin OmpF crystals recorded in aqueous solution by the atomic force microscope (AFM) revealed 15 Å lateral and 1 Å vertical resolution when compared to the atomic structure from X-ray crystallography. Determination of the bilayer and protein surfaces with this precision on both sides allowed protein-protein and lipid-protein interactions to be modeled at atomic scale. Different conformations of the extracellular porin surface demonstrate the potential of the AFM to monitor conformational changes at submolecular resolution.

Tu-PM-C9

ANTIBODY-ANTIGEN UNBINDING FORCES MEASURED BY FORCE MICROSCOPY USING ANTIBODIES BOUND TO AFM TIPS VIA A SPECIALLY DESIGNED FLEXIBLE CROSSLINKER. ((P.Hinterdorfer, H.Gruber, K.Schilcher, W.Baumgartner, Th.Haselgrübler, H.Schindler)) Institute for Biophysics, University of Linz, Austria

Polyclonal antibodies (Ab) against human serum albumin (HSA) were covalently crosslinked to Si_3N_4 AFM tips. The crosslinker was newly synthesized, essentially consisting of a flexible PEG chain (Poly(ethylene glycol), n=18 or 43) with one amine-reactive end for conjugation to functionalized tips and one thiol-reactive end for Ab binding. The antigen (HSA) was covalently linked to freshly cleaved mica sheets using the same crosslinker. Surface densities of both antibody and antigen were adjusted to ~400/μm^2, corresponding to ~one antibody per tip, assayed by novel means of high resolution fluorescence microscopy ("Single Dye Tracing", see Schmidt,Th.,et al, this issue). With a NANOSCOPE III force-distance curves, F(z), were measured during continuous down (trace) and up (retrace) movements of the tip at different fixed lateral positions. At appropriate buffer conditions (see Schilcher,K., this issue) unspecific interactions, especially adhesion, were effectively eliminated. Physical linkage of tip to substrate via antibody-antigen binding was evident from an attractive force which developed during retraces. This attractive force increased from zero (at contact) in a non-linear fashion with increasing distance, consistent with estimates of the stretching force of the PEG chain. At distances roughly corresponding to the effective length of the antibody and the fully streched PEG chain attractive forces jumped to zero reflecting sudden breakage (unbinding force) of the antibody-antigen bond. Binding and unbinding occured reversibly during repetitive trace-retrace cycles (1/sec, usually several 100 cycles at each position). For different preparations of conjugated tips and substrates and for different positions for each substrate the unbinding forces fell consistently into a Gaussian distribution with a mean and SD of (0.4±0.2)nN. Antibody-antigen binding occured sufficiently fast to allow for imaging the distribution of antibody binding sites during area scans, currently under study in application to membranes with identification of ion channels, their distribution and surface topology. (supported by the Austrian Research Funds, project S66/07).

Tu-PM-C10

A NOVEL FLOW INJECTION SYSTEM FOR CELL PERFUSION STUDIES. ((P. J. Baxter, G. D. Christian and J. Ruzicka)) University of Washington, Dept. of Chemistry, Seattle, WA 98195

We have developed a novel and versatile flow injection system capable of flow and sequential injection as well as fluid switching analyses (modes) with minimal hardware reconfiguration.[1] The system consists of two high precision linear syringe pumps and a multiposition selector valve. The combination of the three modes makes the instrument capable of delivering traditional flow injection profiles, square impulses and fast transient (70 ms) pulses over cells in a perfusion chamber. However, the high precision offered by this instrument does not preclude its use for routine analysis. The most salient feature of the system is the ability to generate subsecond pulses and step pulses of reagents - highly desirable features for cell perfusion studies. This versatile fluidic system can be coupled with any existing cell-perfusion chamber. Instrumental capabilities are demonstrated with studies using baby hamster kidney cells with a perfusion chamber developed in our laboratory.[2]

[1] Baxter, P. J.; et al. *Anal. Chem.* **1994** submitted.
[2] Scudder, K. M.; et al. *Anal. Chem.* **1992**, *64*, 2657-2660.

Tu-PM-D1

FORMATION OF 2-D COMPLEXES OF F-ACTIN AND CROSSLINKING PROTEINS ON LIPID MONOLAYERS. ((Kenneth A. Taylor and Dianne W. Taylor)) Dept. of Cell Biology, Duke Univ. Medical Center, Durham, NC 27710. (Spon. by M. Titus)

We have developed a method for forming 2-D paracrystalline complexes of F-actin and bundling/gelation proteins on positively charged lipid monolayers composed of dilaurylphosphatidylcholine and didodecyldimethylammonium bromide. These arrays can be used as 2-D analogs of the 3-D bundles formed in solution to facilitate more detailed structural studies of protein interactions with F-actin by eliminating superposition effects. The method has been applied to the formation of 2-D bundles of F-actin using crosslinkers such as the glycolytic enzymes aldolase and glyceraldehyde-3-phosphate dehydrogenase, the cytoskeletal protein erythrocyte adducin as well as α-actinin from chicken gizzard. All of the 2-D bundles formed contain F-actin with a 13/6 helical structure. Well ordered F-actin-α-actinin 2-D bundles have an interfilament spacing of 36 nm and contain crosslinks 33 nm in length angled ~25-35° to the filament axis. The unit cell of the F-actin-α-actinin bundles contains only a single actin filament thereby demonstrating that chicken gizzard α-actinin can crosslink parallel, unipolar arrays of actin filaments. The crosslinks between α-actinin and the unipolar arrangement of parallel actin filaments lack 2-fold symmetry thereby suggesting at least 2 modes of actin binding. This observation is consistent with an actin crosslinking function for chicken gizzard α-actinin at adhesion plaques where actin filaments are bound to the cell membrane with uniform polarity. Supported by the American Heart Association and NIH grant GM30598.

Tu-PM-D2

EXPRESSION OF CHICKEN BRUSH BORDER MYOSIN-I FRAGMENTS WITH DELETION MUTATIONS OF PUTATIVE CALMODULIN-BINDING SITES. ((M.I.Khoroshev and D.D. Bikle)) Department of Medicine, University of California, San Francisco; Endocrine Unit, Veterans Affairs Medical Center, San Francisco, CA 94121

It has been suggested that brush border myosin-I (BBMI) has up to six potential calmodulin-binding sites, based on the presence of six reasonably well conserved IQ motifs in the mid region of the molecule. It was shown previously from this laboratory that the active metabolite of vitamin D, $1,25(OH)_2D$, increased the calmodulin content of the brush border by increasing calmodulin binding to BBMI in parallel with its ability to increase calcium transport. These data suggest the direct or indirect involvment of the BBMI-calmodulin complex in calcium transport in intestinal cells. Although BBMI has been estimated to bind 3-4 molecules of calmodulin it is unknown whether this ratio of calmodulin to BBMI can vary under different conditions. Likewise it is not known whether all six IQ motifs contribute to calmodulin binding or to the functional activities of BBMI. Here we report that PCR-amplified DNA fragments of BBMI with deletions of one-to-six calmodulin-binding sites and head or tail domains were produced and expressed in an E.coli expression system. Using the calmodulin gel overlay approach we demonstrated that recombinant full length BBMI bound calmodulin. We are currently analyzing sequential deletions of the IQ motifs in order to determine the ability of the different IQ sites to bind calmodulin and regulate BBMI activity.

Tu-PM-D3

ALLOSTERIC DISRUPTION OF *PARAMECIUM* CALMODULIN

((Shawn Harmon and Madeline A. Shea)) Dept. of Biochemistry, U. of Iowa College of Medicine, Iowa City, IA 52242-1109

Functional mutants of *Paramecium* were generated by random mutagenesis, isolated on the basis of altered phenotype and traced to defects in calmodulin (C. Kung, Univ. of Wisconsin-Madison). To determine the nature of calcium-induced transitions between conformational states of *Paramecium* calmodulin (PCaM), eight mutants (distributed in N-terminal (in site II & in the linker between sites I and II) or the C-terminal domains (in sites III & IV and in the last helix)) were compared to wild-type. Calcium-dependent changes in tyrosine fluorescence (primarily reflecting binding at sites III & IV) showed that wild-type PCaM had a higher affinity for calcium than did rat calmodulin. The four N-domain PCaM mutants were nearly identical to wild-type PCaM, unlike C-domain mutants. This is consistent with a model in which sites III and IV have higher affinity for calcium than do sites I and II and properties of each domain alone are the primary determinants of intrinsic affinity. Calcium binding induced an increase in ellipticity; however, the fractional change varied depending on nature and position of mutation. Calcium-dependent differences in the average molecular dimensions of calmodulin were measured by gel permeation chromatography performed under calcium-saturating and apo conditions. The Stokes' radius decreased upon calcium binding; however, the degree of deviation did not fall into domain-specific categories. Stokes' radii of calmodulin-peptide complexes were also measured. Further analysis of the coupling between calcium binding and conformations of these mutants will contribute to understanding pathways of propagated change and the roles these residues play in target activation.

(NSF MCB 9057157, AHA 91014980)

Tu-PM-D4

STRUCTURAL BASIS OF THE PLASTICITY OF Ca^{+2}-CALMODULIN IN MOLECULAR RECOGNITION AND SIGNAL TRANSDUCTION. ((W. E. Meador[1], S. E. George[2], A. R. Means[3] and F. A. Quiocho[1])) [1]Howard Hughes Medical Institute and Department of Biochemistry, Baylor College of Medicine Houston, TX 77030, [2]Department of Cardiology and [3]Department of Pharmacology, Duke University Medical School, Durham, NC 27710

We have determined the x-ray crystal structure of a Ca^{2+}-calmodulin-like chimaeric molecule bound to the calmodulin-binding domain of calmodulin-dependent protein kinase IIα. The chimaera consists of calmodulin in which the central helix has been replaced by the central helix from troponin C. Comparisons with two other structures of complexes of native Ca^{2+}-calmodulin with two target peptides highlight observations of rigid domain structures, target-mediated overall conformation, and central helix pliance in signalling function.

Tu-PM-D5

CALCIUM AND ZINC ION BINDING BY *E. coli* α-HAEMOLYSIN. FUNCTIONAL EFFECTS. ((H. Ostolaza, A. Soloaga and F.M. Goñi)) Department of Biochemistry, University of the Basque Country, P.O. Box 644, 48080 Bilbao, Spain. (Spon. by J.L.R. Arrondo)

α-Haemolysin, an extracellular protein toxin of *E. coli*, is known to disrupt eukaryotic cell membranes. In spite of genetic evidence of Ca^{++} - binding motifs in its sequence, conflicting results are found in the literature on the requirement of divalent cations for the membranolytic activity of the toxin. Moreover, Ca^{++} binding sites have not been characterized to date in the native protein. Our results show that when Ca^{++} levels are kept sufficiently low during bacterial growth and toxin purification, membrane lysis does not occur in the absence of added divalent cations. Ca^{++} and, at higher concentrations, Sr^{++} and Ba^{++}, support the lytic activity, but Mg^{++}, Mn^{++}, Zn^{++}, or Cd^{++} appear to be inactive in this respect. Scatchard analysis of $^{45}Ca^{++}$ binding reveals three equivalent, independent sites, with $K_d \approx 1.1 \times 10^4$ M. No $^{45}Ca^{++}$ binding is observed when the protein is pre-incubated with Zn^{++}. In the light of three-dimensional data available for a structurally related protein, alkaline protease of *Pseudomonas aeruginosa* [Bauman *et al.*, EMBO J. 12, 3357-3364 (1993)] it is suggested that α-haemolysin may bind a larger number of Ca^{++} ions than the three that are more easily exchangeable and are thus detected in the $^{45}Ca^{++}$ binding experiments. In addition, structural similarities and conservation of ion-binding motifs support the hypothesis that His 859 is one of the Zn^{++} ligands.

Tu-PM-D6

TOWARDS AN UNDERSTANDING AT THE MOLECULAR LEVEL OF THE RESPONSE TO CALCIUM BINDING IN EF-HAND PROTEINS. ((W.J. Chazin*, M. Akke, G Carlström, J. Kördel, N.J. Skelton, and B.T. Wimberly)) Department of Molecular Biology, The Scripps Research Institute, La Jolla CA, 92037.

The fine tuning of the conformational response to the binding of Ca^{2+} ions in EF-hand calcium binding proteins (CaBPs) plays a critical role in determining functional properties. Our laboratory utilizes NMR spectroscopy to determine high resolution solution structures of EF-hand CaBPs at various levels of Ca^{2+} loading, thereby directly determining the consequences of ion binding on protein conformation and dynamics. Calbindin D_{9k}, a member of the S-100 subfamily of CaBPs, will be used as a representative example to discuss progress towards our understanding at the molecular level of how the response to ion binding is modulated. Studies of the apo, fully Ca^{2+} loaded and half-saturated states with one ion bound exclusively in either of the two binding sites will be discussed, including detailed comparisons of the high resolution structures of the apo, $(Cd^{2+})_1$ [site II] and $(Ca^{2+})_2$ states. Insights into the basis for the cooperative binding of Ca^{2+} in calbindin D_{9k} have been obtained from these studies and the analysis of the complementary N56A mutant, which binds the first equivalent of Ca^{2+} in site I.

Tu-PM-D7

HIGH RESOLUTION CRYSTAL STRUCTURES OF AMPHIBIAN RED CELL L FERRITIN: A NOVEL MECHANISM FOR IRON UPTAKE.

((J. Trikha[1], E. C. Theil[2] and N. M. Allewell[1])). [1]Department of Biochemistry, University of Minnesota, St. Paul, MN 55108. [2]Department of Biochemistry, North Carolina State University, Box 7622, Raleigh NC 27695.

Ferritins sequester cellular iron in animals, bacteria and plants as ferric oxyhydroxide within a protein shell made of twenty-four subunits with cubic symmetry. There are at least two types of polypeptide chains, H and L, with high sequence homology, but large differences in rates of iron uptake and core formation and their ability to catalyze iron oxidation. We have solved high resolution crystal structures of amphibian red cell L ferritin and a mutant in which Glu 56, 57, 58 and 60 at the proposed iron nucleation site are replaced by Ala that has a reduced rate of iron mineralization under two sets of crystallization conditions. The positions of a linear array of charged residues extending from the three-fold axis, a proposed site of iron uptake, through the proposed nucleation site shift with changes in the ionic environment and as a result of the mutations. Electrostatic modeling indicates that the channel at the three-fold axis is surrounded by a region of negative potential and that channel of negative potential connect this site to the iron oxidation and nucleation sites, providing a potential pathway for movement of iron within the molecule. Supported by NIH grant DK-17335 to NMA.

Tu-PM-D8

ANION RECOGNITION IN AN ALLOSTERIC pH-DRIVEN PHASE TRANSITION IN CUBIC INSULIN CRYSTALS.

((O. Gursky & D. L. D. Caspar, Rosenstiel Basic Medical Sciences Research Center, Brandeis University, Waltham MA 02254))

X-ray diffraction analysis to1.8Å resolution of the phase transition in cubic SO_4-insulin crystals provides new insights into allosteric mechanisms of anion-selective protein reactions. Decease in pH from 6 to 5.7 leads to cooperative SO_4^{2-} binding by rearranged triads of B1-B3 groups linked to close apposition of dyad-related B13 Glu pairs, with a single H^+ shared by the pair via two bridging waters. Binding of $H_2PO_4^-$, which apparently correlates with normal phosphate titration, induces similar reorientation in B1-B3 groups but stabilizes the separated B13 Glu pair conformation by sharing H^+ with the nearby B13 COO^- via bridging water. The structures of selenate- and sulfate-insulin are not isomorphous: at acid pH, lack of localized SeO_4^{2-} binding leads to increased overall crystal disorder, especially in B1 groups; similar, although smaller disorder is observed in Cl-insulin which also displays no localized anion binding. Coupling of sulfate-induced switching movements about the crystal 2- and 3-fold facilitates their propagation throughout the lattice, resulting in an apparent first-order phase transition. Lack of B13 Glu pair switching about the crystal dyad in H_2PO_4-insulin explains the local character of the transition. Differential effect of SeO_4^{2-} and Cl^- on the insulin structure suggests that these mobile anions are localized near the B-chain N-termini. Anion charge, H-bonding capacity, size, and hydration provide the basis for atomic recognition of $H_2PO_4^-$, HPO_4^{2-}, SO_4^{2-}, SeO_4^{2-}, and Cl^- at the cubic insulin site; similar factors should contribute to anion recognition at the solvent accessible sites in the course of antibody-anionic hapten binding, phosphorylation, and many enzymatic reactions. The transition exemplifies how ligand-induced conformational changes can be transmitted in concert by means of short-range interactions between small atomic groups, without any tertiary rearrangements.

Tu-PM-D9

The Three Dimensional Structure of NAD(P)H:(Quinone Acceptor) Oxidoreductase

((R. Li[1], M.A. Bianchet[1], P. Talalay[2], L.M. Amzel[1])) [1]Department of Biophysics and Biophysical Chemistry, [2]Department of Pharmacology and Molecular Sciences, The Johns Hopkins University School of Medicine , Baltimore MD 21205, USA

NAD(P)H:(quinone acceptor) oxidoreductase (quinone reductase or DT-diaphorase) is an FAD-containing protein that catalyzes the obligatory two-electron reduction of quinones by NAD(P)H. The enzyme protects cells against quinone carcinogens by preventing the formation of semiquinone radicals, and may be involved in the vitamin K-dependent blood coagulation cascade. The three dimensional structure of rat liver quinone reductase complexed with Cibacron Blue, a potent inhibitor of the enzyme, has been determined by X-ray crystallography to 2.4 Å resolution. The crystals belong to the monoclinic space group I2 (non-standard setting of C2) with cell dimensions of $a = 72.0$, $b = 107.0$, $c = 88.4$, $\beta = 92.6^o$. There are two molecules in the asymmetric unit related by two-fold non-crystallographic symmetry. The phases were determined by multiple isomorphous replacements with three heavy atom derivatives, and were improved by solvent flattening and density averaging over the non-crystallographic two-fold axis. The molecular structure of this 273-residue globular protein contains two domains, a major amino-terminal α/β structure containing FAD binding site(s), and a small carboxyl terminal of 60 residues. The two monomers related by crystallographic symmetry are in tight contact, and may represent the physiological dimer. *(Supported by NIH Grants GM45540 and GA44530)*

BIOCHEMISTRY AND MECHANICS OF MUSCLE CONTRACTION II

Tu-PM-E1

EFFECT OF CALCIUM ON AMP-PNP BINDING TO MYOSIN IN RABBIT SKELETAL MUSCLE.

((S.M. Frisbie[#], J.M. Chalovich[+], B. Brenner[*] and L.C. Yu[#])) [#]NIH, Bethesda, MD; [+]East Carolina University, Medical School, NC; [*]Medical School Hannover, Germany.

It was previously observed that the affinity of MgATPγS (Kraft et al. 1992, PNAS 89, 11362), and MgGTP (Frisbie and Yu 1994, Biophy. J. 66, A301) for crossbridges was calcium sensitive. To determine whether this calcium sensitivity is a general property of nucleotide binding to attached crossbridges, we have studied the titration of AMP-PNP in skinned rabbit psoas muscle fibers. The binding of MgAMP-PNP (Sigma) to myosin was followed by changes in the x-ray equatorial intensity ratio $[I_{11}]/[I_{10}]$. The nucleotide was increased from 0.1 mM to 40 mM at 0°C, pH = 7.0. Since the pK_a of the terminal phosphate proton is 7.7 for AMP-PNP (Yount et al. 1971, Biochem. 10, 2484), the ionic strength (μ) was adjusted such that the conductivity of the MgAMP-PNP containing solutions was matched to that of the MgATP relaxing solution (μ = 170 mM) by K-proprionate. HPLC analysis showed that there was less than 0.06% contamination by ATP. By adding hexokinase and glucose in the solution, the trace contaminant ATP was removed, such that no evidence of fiber activation was observed throughout the experiments. In the absence of Ca^{+2}, saturation was reached at approximately 15mM of MgAMP-PNP with the intensity ratio being identical to that of relaxed fibers in ATP. However, in the presence of calcium, saturation was not reached even at 40 mM of MgAMP-PNP. The K_m in the presence and absence of Ca^{++} appears to differ by at least 10 fold. Therefore, the results suggest that in the presence of Ca^{+2}, i.e. when the actin filament is activated, the affinity of myosin for nucleotide is generally weaker.

Tu-PM-E2

THE INTERACTION OF ALKALI LIGHT CHAIN 1 WITH F-ACTIN FULLY OR PARTIALLY DECORATED BY MYOSIN SUBFRAGMENT 1.

((O.A. Andreev)) Baylor Research Institute, Dallas, TX 75226.

We found earlier that two different rigor complexes could be formed depending on molar ratio (MR) of myosin subfragment 1 (S1) to actin (Andreev & Borejdo, 1992, J. Muscle Res. Cell Motil. 13:523; Andreeva et al., 1993, Biochem., 32:13956). In the present work the effect of MR on cross-linking with EDC of light chain 1 (LC1) of S1 with actin was examined. To identify the cross-linked products of LC1 with actin or S1, fluorescently labeled LC1 was incorporated into S1. It was found that production of covalent complex of actin with LC1 strongly depended on molar ratio of S1(LC1) to actin. In 8% polyacrylamide tricine gel cross-linked products of S1 with one actin migrated as doublet with apparent molecular weights 150 and 160 KDa and the complex of S1 with two actins migrated as 210 KDa band. When actin was in excess four major fluorescent products were observed with apparent molecular weights 67 KDa (LC1-actin), 120 KDa (LC1-S1), 185 KDa (LC1-actin-S1) and 235 KDa (LC1-actin-S1-actin). When S1 was in excess the only fluorescent product was 120 KDa (LC1-S1). These results indicate that LC1 of S1 does not interact with F-actin fully saturated with S1(LC1). Supported by AHA.

Tu-PM-E3

WATER AND ION INTERACTIONS WITH MYOSIN-ATP HYDROLYSIS INTERMEDIATES

((S. Highsmith)) Biochemistry, UOP, S.F., CA 94115

Myosin subfragment 1 (S1) steady-state MgATPase activity was measured with increasing [ATP] in solutions containing polyethylene glycol (PEG, MW 400 to 6000), trehalose and/or KCl. In the absence of KCl, PEG>400 increased K_M substantially, but not V_{max}. $Log(K_M/K_s)$ decreased linearly with π (osmotic pressure). The slope indicated that 250 water molecules were dissociated to form an inactive S1 species. PEG.400 or trehalose had a negligible effect on K_M. KCl reduced the number of waters involved in the PEG-induced dehydration by 50%. The midpoint was at [KCl] = 20 mM and remained constant from 40 to 220 mM. In the absence of PEG, K_M and V_{max} were decreased 55% by [KCl], with the mid-point at 50 mM.

$$E^* \overset{K_i}{\rightleftarrows} E + S \overset{K_1}{\rightleftarrows} ES \overset{K_2}{\rightleftarrows} E'S \overset{K_3}{\rightleftarrows} EP \overset{k_4}{\rightarrow} E + P$$ (Enzyme; Substrate; Product)

The effect of the large PEG's is to form the dehydrated E*, which cannot bind ATP. If formation of E* involves closing one of S1's crevices, PEG.400 and trehalose may not be effective because they penetrate the crevice(s) reputed to close. Given that K_1 is known to decrease with increasing ionic strength, the decreases in K_M and V_{max} with increasing [KCl] must be due to ion interactions with other species on the pathway. Stabilization of E'S will decrease K_M and V_{max}. (NIH grant PO1AR42895)

Tu-PM-E4

NO EVIDENCE FOR LARGE CHANGES IN FIBER ACTIVATION DURING UNLOADED SHORTENING AND FORCE REDEVELOPMENT.

((B.Brenner & J.M.Chalovich)) Medical School of Hannover, FRG & East Carolina University, USA

The rate constant of isometric force redevelopment, kredev, has been used to characterize cross-bridge turnover kinetics. The use of kredev during partial Ca^{2+} activation was questioned because of possible changes in thin filament activity during shortening when cross-bridges are mostly in weak binding states. We have monitored the state of the actin filament during force redevelopment by following TnI fluorescence. We have shown that the fluorescence of IANBD labeled TnI monitors the extent of activation in skinned psoas fibers. At either low or high levels of Ca^{2+} activation, no changes in fluorescence were observed during the measurement. However, at intermediate levels of activation, there was a small (about 16% of the maximum) change in fluorescence which indicated a slight shift to a less active form of the thin filament. This indicates that a small correction must be applied to the kredev measurements at intermediate levels of activation. However, this correction does not alter pervious conclusions drawn from measurements of force redevelopment at intermediate Ca^{2+} concentrations.
Supported by DFG 849/1-4, NIH, AR40540 and NATO 930448.

Tu-PM-E5

DO WEAKLY BINDING CROSSBRIDGES EXIST?

((Marc L. Bartoo, Wolfgang A. Linke and Gerald H. Pollack))
Center for Bioengineering, University of Washington, Seattle WA 98195.

Single, isolated myofibrils from cardiac and skeletal muscle were used to characterize the visco-elastic passive tension response to dynamic sarcomere-length changes. We attempted to separate the stiffness contribution of the connecting filament from that of weakly bound crossbridges by characterizing the stiffness and stress-relaxation behavior of isolated myofibrils over a wide range of sarcomere lengths. Efforts to enhance weak crossbridge binding by lowering ionic strength were met by clear contractile responses. Even at low temperature, myofibrils bathed in low ionic strength relaxing solution generated increased baseline tension and sarcomere shortening relative to normal ionic strength controls. Thus, increases in stiffness in low ionic strength solution cannot be attributed to weak crossbridge binding, but are instead caused by active contraction. In normal ionic strength solution, myofibrils were subjected to 500 Hz oscillations ranging in amplitude from 2.5 to 80 nm/half sarcomere. A prediction of the weak crossbridge binding hypothesis is that the stiffness response should drop as sarcomeres are stretched beyond the reach of bound bridges. No evidence for such a change was found -- with increasing oscillatory amplitude the stiffness response was linear. In fact, examination of the stiffness response at sarcomere lengths with and without filament overlap showed a consistent relationship between stiffness and the magnitude of isometric passive tension. When passive tension was reduced by damaging connecting filaments, passive stiffness and tension dropped in parallel. We were unable to measure a residual stiffness contribution from weakly binding crossbridges, even at full filament overlap. The consistent relationship between stiffness and passive tension at all sarcomere lengths suggests that a single element is responsible for both. Since passive tension is borne by connecting filaments in isolated myofibrils, it follows that stiffness is also based on connecting filaments.

Tu-PM-E6

DISRUPTION OF MYOSIN LIGHT CHAIN KINASE (MLCK) -DEPENDENT PHOSPHORYLATION SITE ALTERS THE RECRUITMENT OF ACTIVATED CROSS-BRIDGES IN *DROSOPHILA* INDIRECT FLIGHT MUSCLE (IFM).

((H. Yamashita[1], C. Hyatt[1], R. Tohtong[3], A. Simcox[3], J. Vigoreaux[2], J. Haeberle[1], G. Sleeper[1], and D. Maughan[1])) [1]Dept. Molecular Physiology & Biophysics, [2]Dept. Zoology, Univ. of Vermont, Burlington, VT 05405, and [3]Dept. Molecular Genetics, Ohio State University, Columbus, OH 43210.

Drosophila myosin regulatory light chain is phosphorylated at Ser66 and Ser67 by a Ca^{2+}-calmodulin-dependent MLCK. Mutation of these serine residue(s) into alanines (*S66A* and *S66A,S67A*) caused impaired flight ability and decreased wing beat frequency in flies, and depressed maximum power output generated by isolated, demembranated flight muscle fibers (Biophys J. 66(2):A123;1994). We investigated whether the impaired flight muscle function is due to a decreased number of cross-bridges recruited by stretch-activation, altered kinetics of actomyosin interaction, or both. Complex stiffness data obtained from sinusoidal length perturbations were fitted with two exponential processes ***B*** and ***C*** and a frequency-dependent viscoelastic component ***A***. The magnitudes of both ***B*** (related to cross-bridge attachment and responsible for stretch-activation response) and ***C*** (related to cross-bridge detachment) were significantly less in *S66A* single and *S66A,S67A* double substitution mutants as compared to the wild-type control but had unaltered rate constants of ***B*** and ***C***. These results suggest that phosphorylation of Ser66 plays a significant role in the stretch-activation mechanism by regulating the number of activated cross-bridges without changing the kinetics in *Drosophila* IFM. Supported by NIH AR40234.

Tu-PM-E7

NON-UNIFORMITY OF SARCOMERES DURING STRETCH OF ACTIVE MUSCLE AT LONG LENGTH.

((D.L. Morgan, U. Proske, J. Talbot, R. Lynn, T Allen, C. Jones)) Monash University Clayton, Vic. 3168, Australia.

Extremely nonuniform lengthening of sarcomeres has been postulated during stretch of active muscle on the descending limb of the length tension curve. (Morgan 1990 Biophys J, 57, 209-221) The supporting evidence was then mainly indirect, through explanations for a number of observations which are otherwise difficult to explain. Since then, considerable extra evidence has been acquired. Electron microscopy of muscles fixed while still active after a stretch has shown sarcomeres with no filament overlap in one half, in sufficient numbers to account for at least half of the applied stretch. Such sarcomeres were absent from muscles fixed during an isometric contraction and largely absent from muscles stretched on the ascending limb of the length-tension curve. A series of eccentric contractions has been shown to shift the muscle length for maximum tension generation to longer lengths in both toad and human muscle, consistent with loss of interdigitation in some sarcomeres. As predicted, the shift is greater at longer muscle lengths and for larger stretches, but is independent of speed. After a few hours in both isolated toad muscle and intact human triceps surae, the optimum length returned to its original value. E-m of toad muscle after a series of eccentric contractions has shown different sized areas of overextended sarcomeres. Several hours after the last contraction, the small, but not the large, areas returned to normal. Finally, the increase in the number of sarcomeres, postulated as the basis for the training effect of eccentric exercise, has been shown in rats exercised by incline and decline running on a treadmill.

Tu-PM-E8

INDIRECT COUPLING OF PHOSPHATE RELEASE AND *DE NOVO* TENSION GENERATION DURING MUSCLE CONTRACTION.

((J.S. Davis and M.E. Rodgers)) Department of Biology, The Johns Hopkins University, 34th and Charles Streets, Baltimore, MD 21218.

A key question in muscle contraction is how the chemistry of the actomyosin ATPase is coupled to the mechanics of tension generation. Both phosphate release and the kinetics of phase 2_{slow}, a mechanical step seen in length-jump experiments, are considered closely linked to tension generation. We determined their interrelationship by examining the effect of phosphate on the two-step mechanism of tension generation seen in laser temperature-jump experiments of skinned rabbit psoas fibers. Phosphate introduces a new relaxation ($1/\tau_{negative}$) which reduces tension and is the equivalent of the Huxley-Simmons phase 3 in length-jump experiments where it causes a reversal of the return to the pre-jump isometric tension. By contrast, phosphate has little effect on medium ($1/\tau_2$) and slow ($1/\tau_3$) relaxations correlated, respectively, with *de novo* tension generation and a rate-limiting step. We conclude that phosphate release is separated from tension generation by an irreversible conformational change of a cross-bridge ADP state. The tension-generating conformational change is thus indirectly coupled to phosphate release.
Supported by NIH grant AR-04349 to J.S.D.